



Article

Uranoclite, a new uranyl chloride mineral from the Blue Lizard mine, San Juan County, Utah, USA

Anthony R. Kampf^{1*} , Jakub Plášil², Travis A. Olds³, Barbara P. Nash⁴ and Joe Marty⁵

¹Mineral Sciences Department, Natural History Museum of Los Angeles County, 900 Exposition Boulevard, Los Angeles, CA 90007, USA; ²Institute of Physics ASCR, v.v.i., Na Slovance 1999/2, 18221 Prague 8, Czech Republic; ³Section of Minerals and Earth Sciences, Carnegie Museum of Natural History, 4400 Forbes Avenue, Pittsburgh, Pennsylvania 15213, USA; ⁴Department of Geology and Geophysics, University of Utah, Salt Lake City, UT 84112, USA; and ⁵5199 East Silver Oak Road, Salt Lake City, UT 84108, USA

Abstract

The new mineral uranoclite (IMA2020-074), $(\text{UO}_2)_2(\text{OH})_2\text{Cl}_2(\text{H}_2\text{O})_4$, was found in the Blue Lizard mine, San Juan County, Utah, USA, where it occurs as tightly intergrown aggregates of irregular yellow crystals in a secondary assemblage with gypsum. The streak is very pale yellow and the fluorescence is bright green–white under 405 nm ultraviolet light. Crystals are translucent with vitreous lustre. The tenacity is brittle, the Mohs hardness is $\sim 1\frac{1}{2}$, the fracture is irregular. The mineral is soluble in H_2O and has a calculated density of $4.038 \text{ g}\cdot\text{cm}^{-3}$. Electron microprobe analyses provided $(\text{UO}_2)_2(\text{OH})_{2.19}\text{Cl}_{1.81}(\text{H}_2\text{O})_4$. The six strongest powder X-ray diffraction lines are $[d_{\text{obs}} \text{ \AA}(I)(hkl)]: 8.85(38)(002), 5.340(100)(200, 110), 5.051(63)(\bar{2}02), 4.421(83)(112, 004, 202), 3.781(38)(\bar{2}12)$ and $3.586(57)(014, \bar{2}04)$. Uranoclite is monoclinic, $P2_1/n$, $a = 10.763(8)$, $b = 6.156(8)$, $c = 17.798(8) \text{ \AA}$, $\beta = 95.656(15)^\circ$, $V = 1173.5(18) \text{ \AA}^3$ and $Z = 4$. The structure is the same as that of synthetic $(\text{UO}_2)_2(\text{OH})_2\text{Cl}_2(\text{H}_2\text{O})_4$ in which the structural unit is a dimer consisting of two pentagonal bipyramids that share an equatorial OH–OH edge. The dimers are linked to one another only by hydrogen bonding. This is the second known uranyl mineral containing essential Cl and the first in which Cl coordinates to U^{6+} .

Keywords: uranoclite, new mineral, uranyl chloride, crystal structure, Raman spectroscopy, Blue Lizard mine, Red Canyon, Utah, USA

(Received 30 January 2020; accepted 26 March 2020; Accepted Manuscript published online: 31 March 2020; Associate Editor: Sergey V. Krivovichev)

Introduction

The Blue Lizard mine in Red Canyon, Utah, is now well known as a prolific source of new minerals and particularly for its many Na uranyl sulfates. Of the 22 new minerals described from this mine, all are sulfates, 16 are Na uranyl sulfates and three are uranyl sulfates that do not contain essential Na. The new mineral uranoclite, $(\text{UO}_2)_2(\text{OH})_2\text{Cl}_2(\text{H}_2\text{O})_4$, described herein, is the first new mineral described from the Blue Lizard mine that is not a sulfate. Notably, it also does not contain essential Na. Uranoclite is only the second known uranyl mineral containing essential Cl, the first being blue-lizardite, $\text{Na}_7(\text{UO}_2)(\text{SO}_4)_4\text{Cl}$ (Plášil *et al.*, 2014), which was also first described from the Blue Lizard mine. Interestingly, Cl plays very different roles in the structures of these two minerals.

Uranoclite is named for its composition. It is the first uranyl chloride mineral that contains no other anions other than hydroxyl. The phase has previously been synthesised and its chemical name is di- μ -hydroxido-bis[di-aqua-chlorido-dioxido-uranium(VI)] (Huys *et al.*, 2010). The new mineral and name were approved by the Commission on New Minerals, Nomenclature and Classification of the International Mineralogical Association (IMA2020-074, Kampf *et al.*, 2021). The description is based on

two cotype specimens, both micromounts, deposited in the collections of the Natural History Museum of Los Angeles County, 900 Exposition Boulevard, Los Angeles, CA 90007, USA, catalogue numbers 75101 and 75102.

Occurrence

Uranoclite was found in efflorescent crusts on mine walls underground in the Blue Lizard mine ($37^\circ 33' 26''\text{N}$, $110^\circ 17' 44''\text{W}$), Red Canyon, White Canyon District, San Juan County, Utah, USA. The mine is $\sim 72 \text{ km}$ west of the town of Blanding, Utah, and $\sim 22 \text{ km}$ southeast of Good Hope Bay on Lake Powell. Detailed historical and geological information on the Blue Lizard mine is described elsewhere (e.g. Kampf *et al.*, 2015a), and is primarily derived from a report by Chenoweth (1993). Abundant secondary uranium mineralisation in Red Canyon is associated with post-mining oxidation of asphaltum-rich sandstone beds laced with uraninite and sulfides in the damp underground environment. Uranoclite is a very rare mineral in the secondary mineral assemblages of the Blue Lizard mine. It occurs with gypsum on matrix comprised mostly of subhedral to euhedral, equant quartz crystals that are recrystallised counterparts of the original grains of the sandstone.

Morphology, physical properties and optical properties

Uranoclite occurs as tightly intergrown aggregates of irregular yellow crystals (Fig. 1). The streak is very pale yellow and the

*Author for correspondence: Anthony R. Kampf, Email: akampf@nhm.org

Cite this article: Kampf A.R., Plášil J., Olds T.A., Nash B.P. and Marty J. (2021) Uranoclite, a new uranyl chloride mineral from the Blue Lizard mine, San Juan County, Utah, USA. *Mineralogical Magazine* 85, 438–443. <https://doi.org/10.1180/mgm.2021.33>

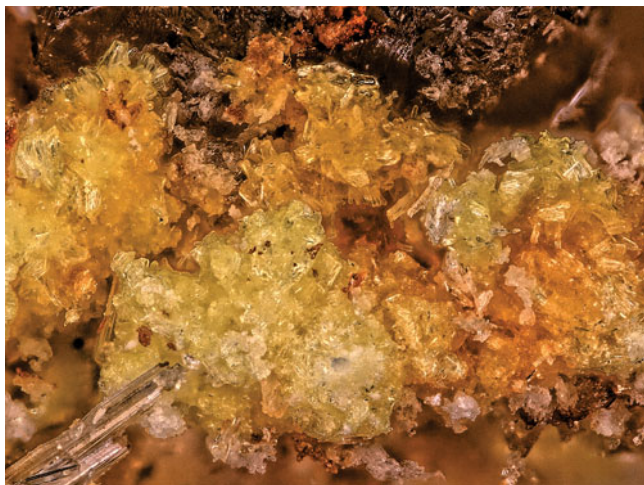


Fig. 1. Tightly intergrown uranocite crystals with gypsum. The field of view is 1.14 mm across.

fluorescence is bright green–white under 405 nm ultraviolet light. Crystals are translucent with vitreous lustre. The tenacity is brittle and the fracture is irregular. The mineral is very soft, probably having a Mohs hardness of $\sim 1\frac{1}{2}$. Multiple cleavages are likely but are impossible to define because of the irregular shape of the crystals and their occurrence in intergrowths. The density could not be measured because the mineral is soluble in Clerici solution and there is insufficient material available for physical measurement. The calculated density based upon the empirical formula is $4.038 \text{ g}\cdot\text{cm}^{-3}$. The mineral is soluble in H_2O at room temperature. The occurrence of the mineral in aggregates of small, poorly formed, translucent crystals made the measurement of optical properties impossible. The Gladstone–Dale relationship using $k(\text{UO}_3) = 0.118$, as provided by (Mandarino, 1976), predicts an average index of refraction of 1.660.

Raman spectroscopy

Raman spectroscopy was conducted on a Horiba XploRA PLUS using a $100\times$ (0.9 NA) objective. The spectrum from 4000 to 60 cm^{-1} obtained using a 532 nm diode laser, 100 μm slit and

2400 gr/mm diffraction grating is shown in Fig. 2. The spectrum from 2000 to 60 cm^{-1} obtained using a 785 nm diode laser, 100 μm slit and 1800 gr/mm diffraction grating is shown in Fig. 3.

As far as we know, no reliable vibrational spectroscopy assignments exist in the literature for synthetic uranyl hydroxide chloride phases, except those of Bullock and Parret (1970), for instance. Thus, the following assignments are based primarily upon those for uranyl oxide hydroxide hydrate (UOH) minerals from Čejka (1999) and Frost *et al.* (2007). All bands in the spectra were fitted using pseudo-Voigt peak profiles.

In the spectrum obtained using a 532 nm laser, three weak bands with centres at 3606, 3539 and 3366 cm^{-1} are assigned to ν (OH) stretching vibrations. Using the empirically derived equation of Libowitzky (1999), the calculated $\text{O}\cdots\text{O}$ distances of the corresponding hydrogen bonds are between $\sim 3.1 \text{ \AA}$ and $\sim 2.8 \text{ \AA}$, in reasonable agreement with refined $\text{O}\cdots\text{O}/\text{Cl}$ bond lengths determined from the structure refinement. We observed no bands related to ν (OH) stretching vibrations in the high wavenumber region of the spectrum using the 785 nm laser; however, a series of broad and very weak bands related to the ν_2 (δ) bending vibrations of H_2O groups are present from ~ 1680 to 1640 cm^{-1} . The additional noisy, broad and very weak bands spanning from ~ 1530 to $\sim 1600 \text{ cm}^{-1}$ are possibly related to bending modes (δ) of U–OH bonds with overlap of ν_2 (δ) H_2O vibrations from the four crystallographically unique H_2O groups in the structure. Strong fluorescence in the 532 nm spectrum prevented detailed analysis of the bands in this region and the remaining assignments have been made using the fitted bands of the 785 nm spectrum.

A complex series of bands between ~ 1400 and $\sim 1000 \text{ cm}^{-1}$ are assigned tentatively as bending vibrations (δ) U–OH of the bridging hydroxyl groups, possibly overlain with overtones or combination bands. The bands of highest intensity in this region are centred near 1226, 1189, and include a moderately intense and complex doublet near ~ 1040 and 1005 cm^{-1} . These assignments are in line, for instance, with multiple bands observed in this range related to (δ) U–OH, librations of H_2O and overtones, found in the calculated spectra of uranopilite (Colmenero *et al.*, 2020). Previously, these bands were generally assigned to stretching modes of SO_4 tetrahedra.

The extremely weak band centred at 910 cm^{-1} is assigned to the $\nu_3(\text{UO}_2)^{2+}$ antisymmetric stretching vibration, while the

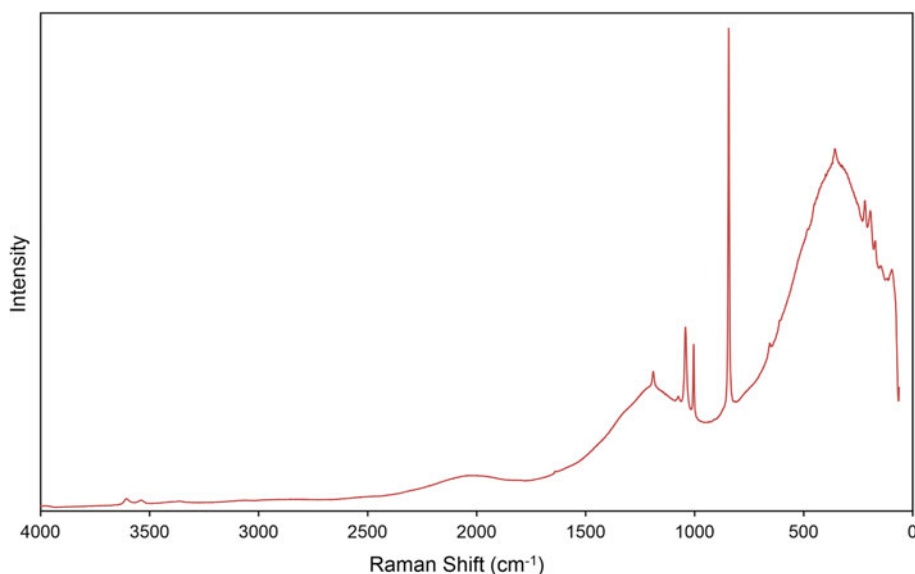


Fig. 2. The Raman spectrum of uranocite recorded with a 532 nm laser. Because of significant fluorescence in the lower wavenumber portion of the spectrum, band assignments in this region are based on the spectrum recorded with a 785 nm laser (Fig. 3).

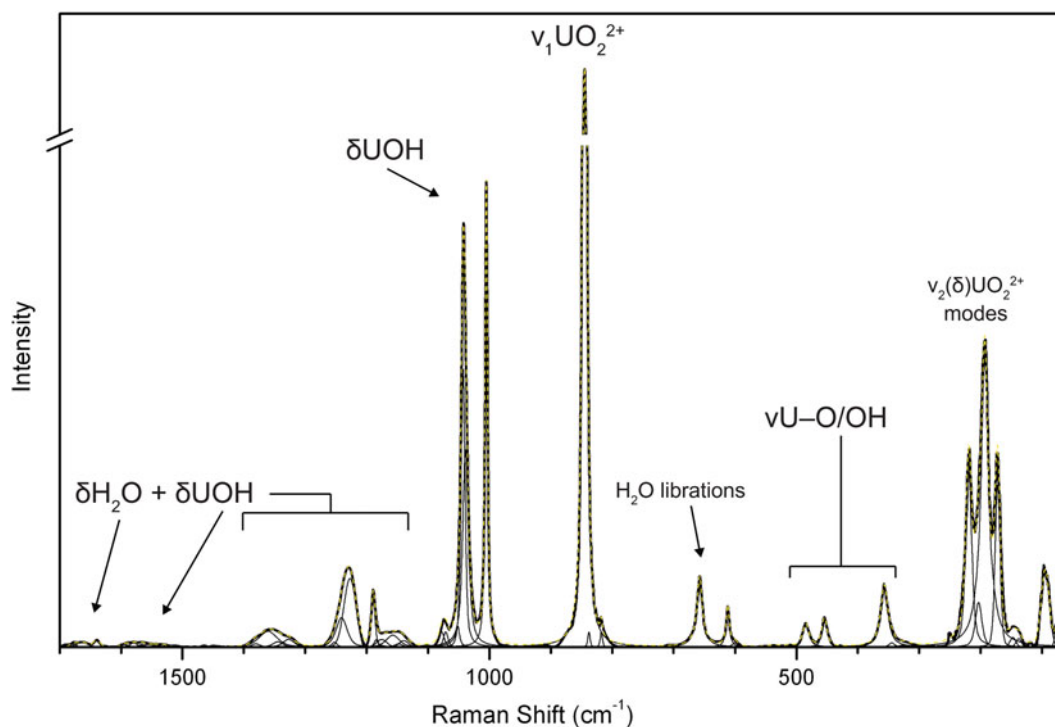


Fig. 3. The baseline corrected and fitted Raman spectrum of uranocite recorded with a 785 nm laser.

$\nu_1(\text{UO}_2)^{2+}$ symmetric stretching vibration occurs as a very strong band at 845 cm^{-1} . Bartlett and Cooney (1989) provided an empirical relationship to determine the approximate U–O_{Ur} bond lengths from the band position assigned to the UO_2^{2+} stretching vibrations, which gives 1.76 \AA (ν_1) and 1.76 (ν_3), in excellent agreement with the average U–O_{Ur} bond lengths from the X-ray data: 1.77 \AA . Frost *et al.* (2005) provide band positions for $\nu_1(\text{UO}_2)^{2+}$ in the synthetic analogue of uranocite, stating: “Another example is $[(\text{UO}_2)_2(\text{OH})_2\text{Cl}_2(\text{H}_2\text{O})_4]$, with two distinct uranium atoms in the unit cell and 847.5s , 850s , 852sh , 855vww (Raman) and 851ms , sharp, 873sh , 883m cm^{-1} (IR)”; however, no further information is provided and we have located no studies examining the synthetic phase by Raman or IR. The reported band positions are comparable to those observed for uranocite; however, despite the presence of two symmetrically distinct uranyl groups, the splitting of $\nu_1(\text{UO}_2)^2$ observed by Frost was not encountered in the spectrum of uranocite.

A pair of weak bands at 657 and 611 cm^{-1} probably arises due to libration modes of H_2O groups, and those at 484 and 454 cm^{-1} to stretching modes of equatorial U–O bonds or librations of H_2O as well. In other UOH minerals with uranyl hydroxide sheets, the bands near $400\text{--}350\text{ cm}^{-1}$ are related to various stretching modes of the equatorial OH and O atoms, and the band at 356 cm^{-1} is assigned as such. A distinct triplet of bands with fitted centres at 219 , 193 and 172 cm^{-1} may be attributed to $\nu_2(\delta)$ (UO_2)²⁺ bending vibrations and unassigned phonon modes.

Chemical composition

Electron probe microanalyses (6 points on 3 crystals) were performed at the University of Utah on a Cameca SX-100 electron microprobe with four wavelength dispersive spectrometers and using *Probe for EPMA* software. Analytical conditions were 15 kV accelerating voltage, 12 nA beam current and $10\text{ }\mu\text{m}$

Table 1. Chemical composition of uranocite.

Constituent	Mean	Range	S.D.	Standard
UO_3	79.58	78.22–80.83	1.06	syn. UO_2
Cl	8.95	8.73–9.17	0.15	tugtupite
H_2O^*	12.77			
O = Cl	–2.02			
Total	99.28			

*Based upon the known stoichiometry (U = 2 apfu, O+Cl = 12 apfu).
S.D. – standard deviation

beam diameter. Raw X-ray intensities were corrected for matrix effects with a $\phi\rho(z)$ algorithm (Pouchou and Pichoir, 1991). No other elements were detected. Crystals took a poor polish, but there was minimal beam damage. Because insufficient material is available for a direct determination of H_2O , it has been

Table 2. Structure details for synthetic $(\text{UO}_2)_2(\text{OH})_2\text{Cl}_2(\text{H}_2\text{O})_4$ (Huys *et al.*, 2010).

Crystal system: Monoclinic					
Space group: $P2_1/n$					
$a = 10.712(2)$	$b = 6.11212(12)$	$c = 17.662(4)\text{ \AA}$			
$\beta = 95.47(3)^\circ$	$V = 1152.8(4)\text{ \AA}^3$	$Z = 4$			
Bond lengths (\AA)		Hydrogen bonds			
U1–O1	1.746(10)	U2–O6	1.759(9)	O3...Cl1	3.62(1)
U1–O2	1.789(10)	U2–O5	1.772(9)	O3...Cl2	3.11(1)
U1–O10	2.367(9)	U2–O9	2.366(10)	O4...Cl1	3.28(1)
U1–O9	2.382(9)	U2–O10	2.373(9)	O4...Cl2	3.23(1)
U1–O3	2.397(9)	U2–O8	2.396(10)	O7...O1	3.35(1)
U1–O4	2.490(10)	U2–O7	2.488(10)	O7...O6	3.03(1)
U1–Cl1	2.751(3)	U2–Cl2	2.772(3)	O8...O2	3.33(1)
				O8...Cl1	3.08(1)
				O9...O5	2.87(1)
				O10...O2	2.80(1)

Table 3. Bond-valence analysis. Values are in valence units.

	U1	U2	Donated H bonds	Accepted H bonds	Sum	
O1	1.89			0.09	1.98	O
O2	1.72			0.18, 0.09	1.99	O
O3	0.48		-0.22, -0.10		0.16	H ₂ O
O4	0.39		-0.18, -0.17		0.04	H ₂ O
O5		1.78		0.16	1.94	O
O6		1.83		0.13	1.96	O
O7		0.39	-0.13, -0.09		0.17	H ₂ O
O8		0.48	-0.24, -0.09		0.15	H ₂ O
O9	0.49	0.51	-0.16		0.84	OH
O10	0.51	0.50	-0.18		0.83	OH
Cl1	0.44			0.24, 0.17, 0.10	0.95	Cl
Cl2		0.41		0.22, 0.18	0.81	Cl
Sum	5.92	5.90				

U⁶⁺-O bond-valence parameters are from Gagné and Hawthorne (2015). U⁶⁺-Cl bond-valence parameters are from Zachariassen (1978). Hydrogen-bond strengths for O-H...O bonds are based on O-O distances using the relation of Ferraris and Ivaldi (1988). Hydrogen-bond strengths for O-H...Cl bonds are based on H-Cl bond lengths using figure 2 in Malcherek and Schlüter (2007); note that H-Cl bond lengths were approximated by subtracting 1.0 Å from the O-Cl distance.

calculated based upon the known stoichiometry (U = 2 atoms per formula unit, O+Cl = 12 apfu). Analytical data are given in Table 1. The empirical formula is (UO₂)₂(OH)_{2.19}Cl_{1.81}(H₂O)₄. The ideal formula is (UO₂)₂(OH)₂Cl₂(H₂O)₄, which requires UO₃ 79.78, Cl 9.89, H₂O 12.56, O = Cl -2.23, total 100 wt.%.

X-ray crystallography

The small size, poor quality and intergrown nature of uranoclite crystals made a single-crystal X-ray diffraction study impossible. Powder X-ray diffraction (PXRD) data were recorded using a Rigaku R-Axis Rapid II curved imaging plate microdiffractometer with monochromatised MoK α radiation. A Gandolfi-like motion on the φ and ω axes was used to randomise the sample. The

pattern provides an excellent match (Fig. 3) with that calculated from the structure of synthetic (UO₂)₂(OH)₂Cl₂(H₂O)₄ determined by Huys *et al.* (2010). Observed *d* values and intensities were derived by profile fitting using *JADE Pro* software (Materials Data, Inc.). Data are given in Supplementary Table S1.

Uranoclite is monoclinic with space group *P2₁/n*. The unit-cell parameters refined from the powder data using *JADE Pro* with whole pattern fitting are *a* = 10.763(8), *b* = 6.156(8), *c* = 17.798(8) Å, β = 95.656(15)° and *V* = 1173.5(18) Å³ (*Z* = 4).

Description of the structure

The crystal structure of uranoclite is presumed to be the same as that of synthetic (UO₂)₂(OH)₂Cl₂(H₂O)₄ (Huys *et al.*, 2010), as is clearly indicated by the close match between the PXRD of uranoclite and that calculated from the structure of the synthetic material. Some of the important details of the structure of synthetic (UO₂)₂(OH)₂Cl₂(H₂O)₄ and a bond-valence analysis, are provided in Tables 2 and 3. Henceforth, to simplify the wording, we will refer to this as the structure of uranoclite.

The most common coordination polyhedron for U⁶⁺ is a squat pentagonal bipyramid in which the apical vertices are the O atoms of the UO₂²⁺ uranyl group and the equatorial vertices are also O atoms that form longer bonds to U. In the structure of uranoclite, one of the equatorial vertices of each uranyl pentagonal bipyramid is a Cl anion. This is very unusual among uranyl phases and has not been reported previously in any mineral structures, although in nollmotzite (Plášil *et al.*, 2018), F occurs as a ligand in two different U⁶⁺ coordinations. The structural unit in uranoclite consists of two pentagonal bipyramids that share an equatorial OH-OH edge forming a dimer with the same formula as the mineral itself, (UO₂)₂(OH)₂Cl₂(H₂O)₄ (Fig. 4). The Cl anions in the dimer are in a *trans* configuration, possibly arranged so due to steric constraints of the large Cl anions. There is no interstitial complex in the structure; the dimers are linked to one another only by hydrogen bonding (Fig. 5).

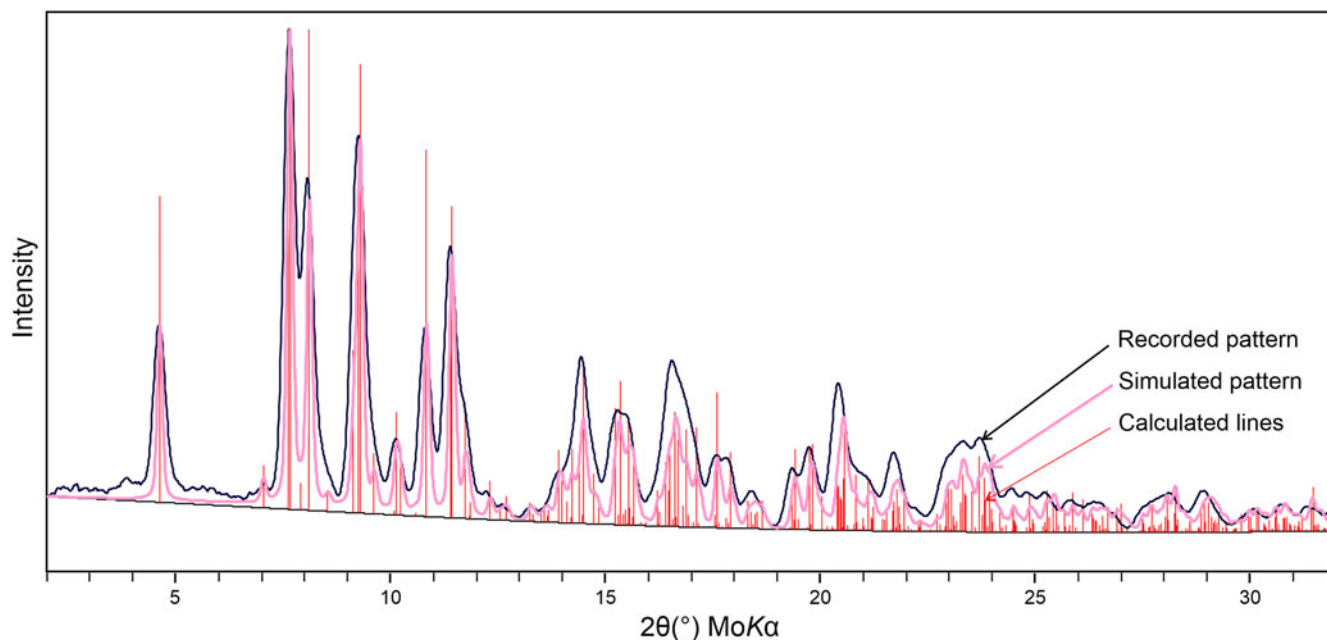


Fig. 4. Powder X-ray diffraction pattern for uranoclite compared with the lines and simulated pattern calculated from the structure of synthetic (UO₂)₂(OH)₂Cl₂(H₂O)₄ (Huys *et al.*, 2010).

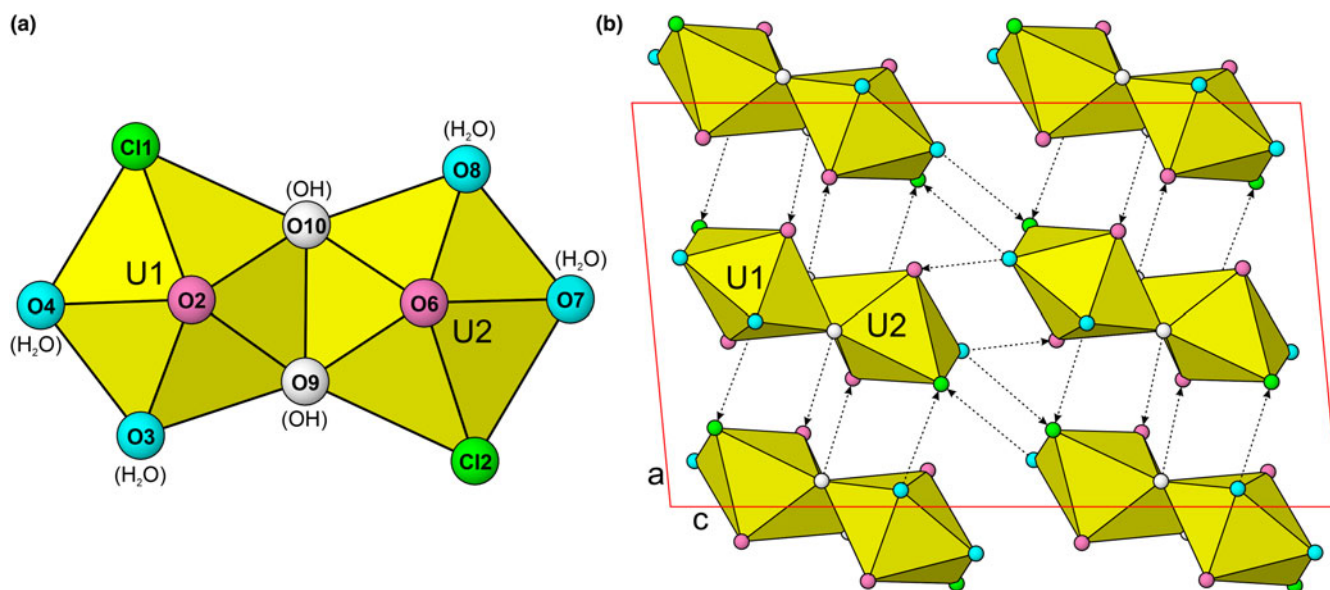


Fig. 5. (a) The $[(\text{UO}_2)_2(\text{OH})_2\text{Cl}_2(\text{H}_2\text{O})_4]$ dimer in uranoclite and the synthetic analogue (Huys *et al.*, 2010). Note the colour coding of O, OH, H_2O and Cl ligands. (b) The crystal structure of uranoclite viewed down $[010]$. Hydrogen bonds are shown as dashed lines with arrows indicating their direction (donor \rightarrow receptor). The unit cell is outlined in red. Ligands are colour coded as indicated in (a). The drawing is based on the structure determination for synthetic $(\text{UO}_2)_2(\text{OH})_2\text{Cl}_2(\text{H}_2\text{O})_4$ (Huys *et al.*, 2010).

The cluster in the structure of uranoclite is of the U_2L_0 -type of Lussier *et al.* (2016). While there are other mineral structures containing dimers composed of two edge-sharing $\text{U}\phi_7$ pentagonal bipyramids, such dimers are generally linked by other polyhedra (e.g. SO_4 tetrahedra) to form larger structural units, such as the sheets of phosphuranylite anion topology (Burns, 2005) found in plášilite (Kampf *et al.*, 2015b) and several other recently described Red Canyon minerals.

Acknowledgements. Sergey Aksenov and an anonymous reviewer are thanked for their constructive comments on the manuscript. We are grateful to retired miner Dan Shumway of Blanding, Utah, for advice and assistance in our collecting efforts in Red Canyon. Funding to JP was provided by the Czech Science Foundation (20-11949S). This study was also funded by the John Jago Trelawney Endowment to the Mineral Sciences Department of the Natural History Museum of Los Angeles County.

Supplementary material. To view supplementary material for this article, please visit <https://doi.org/10.1180/mgm.2021.33>

References

- Bartlett J.R. and Cooney R.P. (1989) On the determination of uranium-oxygen bond lengths in dioxouranium(VI) compounds by Raman spectroscopy. *Journal of Molecular Structure*, **193**, 295–300.
- Bullock J.I. and Parret F.W. (1970) The low frequency infrared and Raman spectroscopic studies of some uranyl complexes: the deformation frequency of the uranyl ion. *Canadian Journal of Chemistry*, **48**, 3095–3097.
- Burns P.C. (2005) U^{6+} minerals and inorganic compounds: Insights into an expanded structural hierarchy of crystal structures. *The Canadian Mineralogist*, **43**, 1839–1894.
- Čejka J. (1999) Infrared spectroscopy and thermal analysis of the uranyl minerals. Pp. 521–622 in: *Uranium: Mineralogy, Geochemistry and the Environment* (P.C. Burns and R.C. Ewing, editors). Reviews in Geochemistry, Vol. 38. Mineralogical Society of America, Washington D.C.
- Chenoweth W.L. (1993) The Geology and Production History of the Uranium Deposits in the White Canyon Mining District, San Juan County, Utah. *Utah Geological Survey Miscellaneous Publication*, 93–3.
- Colmenero, F., Plášil J., Timón V. and Čejka J. (2020) Full crystal structure, hydrogen bonding and spectroscopic, mechanical and thermodynamic properties of mineral uranopilite. *RSC Advances*, **10**, 31947.
- Frost R.L., Weier M.L., Martens W.N., Kloprogge J.T. and Kristóf J. (2005) Thermo-raman spectroscopic study of the uranium mineral subugalite. *Journal of Raman Spectroscopy*, **36**, 797–805.
- Frost R.L., Čejka J. and Weier M.L. (2007) Raman spectroscopic study of the uranyl oxyhydroxide hydrates: Becquerelite, billietite, curite, schoepite and vandendriesscheite. *Journal of Raman Spectroscopy*, **38**, 460–466.
- Gagné O.C. and Hawthorne F. (2015) Comprehensive derivation of bond-valence parameters for ion pairs involving oxygen. *Acta Crystallographica*, **B71**, 562–578.
- Huys D., Van Deun R., Pattison P., Van Meervelt L. and Van Hecke K. (2010) Redetermination of di- μ -hydroxido-bis [diaquachloridodioxidouranium (VI)] from single-crystal synchrotron data. *Acta Crystallographica*, **E66**, i11.
- Kampf A.R., Plášil J., Kasatkin A.V., Marty J. and Čejka J. (2015a) Fermitte, $\text{Na}_4(\text{UO}_2)(\text{SO}_4)_3 \cdot 3\text{H}_2\text{O}$ and oppenheimerite, $\text{Na}_2(\text{UO}_2)(\text{SO}_4)_2 \cdot 3\text{H}_2\text{O}$, two new uranyl sulfate minerals from the Blue Lizard mine, San Juan County, Utah, USA. *Mineralogical Magazine*, **79**, 1123–1142.
- Kampf A.R., Kasatkin A.V., Čejka J. and Marty J. (2015b) Plášilite, $\text{Na}(\text{UO}_2)(\text{SO}_4)(\text{OH}) \cdot 2\text{H}_2\text{O}$, a new uranyl sulfate mineral from the Blue Lizard mine, San Juan County, Utah, USA. *Journal of Geosciences*, **60**, 1–10.
- Kampf A.R., Plášil J., Olds T.A., Nash B.P. and Marty J. (2021) Uranoclite, IMA 2020-074. CNMNC Newsletter 59; *Mineralogical Magazine*, **85**, 278–281, <https://doi.org/10.1180/mgm.2021.5>
- Libowitzky E. (1999) Correlation of O-H stretching frequencies and O-H...O hydrogen bond lengths in minerals. *Monatshefte für Chemie*, **130**, 1047–1059.
- Lussier A.J., Lopez R.A. and Burns P.C. (2016) A revised and expanded structure hierarchy of natural and synthetic hexavalent uranium compounds. *The Canadian Mineralogist*, **54**, 177–283.
- Mandarino J.A. (1976) The Gladstone-Dale relationship – Part 1: derivation of new constants. *The Canadian Mineralogist*, **14**, 498–502.

- Plášil J., Kampf A.R., Kasatkin A.V. and Marty J. (2014) Bluelizardite, $\text{Na}_7(\text{UO}_2)(\text{SO}_4)_4\text{Cl}(\text{H}_2\text{O})_2$, a new uranyl sulfate mineral from the Blue Lizard mine, San Juan County, Utah, USA. *Journal of Geosciences*, **59**, 145–158.
- Plášil J., Kampf A.R., Škoda R. and Čejka J. (2018) Nollmotzite, $\text{Mg}[\text{U}^{\text{V}}(\text{U}^{\text{VI}}\text{O}_2)_2\text{O}_4\text{F}_3] \cdot 4\text{H}_2\text{O}$, the first natural uranium-oxide containing fluorine. *Acta Crystallographica*, **B74**, 362–369.
- Pouchou J.-L. and Pichoir F. (1991) Quantitative Analysis of Homogeneous or Stratified Microvolumes Applying the Model “PAP.” Pp. 31–75 in: *Electron Probe Quantitation*. Springer US, Boston, MA.
- Zachariasen W.H. (1978) Bond lengths in oxygen and halogen compounds of *d* and *f* elements. *Journal of Less Common Metals*, **62**, 1–7.